Received: 24 December 2020 | Revised: 3 February 2021 | Accepted: 5 February 2021

DOI: 10.1096/fj.202002778R

RESEARCH ARTICLE

THE FASEB JOURNAL

Targeting alveolar-specific succinate dehydrogenase A attenuates pulmonary inflammation during acute lung injury

Christine U. Vohwinkel[1] | Ethan J. Coit[1] | Nana Burns[1] | Hanan Elajaili[1] | Daniel Hernandez-Saavedra[2] | Xiaoyi Yuan[3] | Tobias Eckle[4] | Eva Nozik[1] | Rubin M. Tuder[2] | Holger K. Eltzschig[3]

[1]Developmental Lung Biology, Cardiovascular Pulmonary Research Laboratories, Division of Pulmonary Sciences and Critical Care Medicine, Division of Pediatric Critical Care, Departments of Medicine and Pediatrics, University of Colorado, Aurora, CO, USA

[2]Division of Pulmonary Sciences and Critical Care Medicine, University of Colorado, Aurora, CO, USA

[3]Department of Anesthesiology, McGovern Medical School, The University of Texas Health Science Center at Houston, Houston, TX, USA

[4]Department of Anesthesiology, University of Colorado - Anschutz Medical Campus, Aurora, CO, USA

Correspondence

Christine U. Vohwinkel, Developmental Lung Biology, Cardio Vascular Pulmonary Research Laboratories, Division of Pulmonary Sciences and Critical Care Medicine, Division of Pediatric Critical Care, Departments of Medicine and Pediatrics, University of Colorado, Anschutz Medical Campus, Aurora, CO, USA.
Email: Christine.Vohwinkel@cuanschutz.edu

Funding information

HHS | NIH | National Institute of Child Health and Human Development (NICHD), Grant/Award Number: K12HD068372; HHS | NIH | National Heart, Lung, and Blood Institute (NHLBI), Grant/Award Number: K08HL130586; Parker B Francis Foundation, Grant/Award Number: Parker B Francis Fellowship; HHS | NIH | National Heart, Lung, and Blood Institute (NHLBI), Grant/Award Number: R01HL133900; HHS | NIH | National Institute of Diabetes and Digestive and Kidney Diseases (NIDDK), Grant/Award Number: R01DK122796; HHS | NIH | National Institute of Diabetes and Digestive and Kidney Diseases (NIDDK), Grant/Award Number:

Abstract

Acute lung injury (ALI) is an inflammatory lung disease, which manifests itself in patients as acute respiratory distress syndrome (ARDS). Previous studies have implicated alveolar-epithelial succinate in ALI protection. Therefore, we hypothesized that targeting alveolar succinate dehydrogenase SDH A would result in elevated succinate levels and concomitant lung protection. Wild-type (WT) mice or transgenic mice with targeted alveolar-epithelial *Sdha* or hypoxia-inducible transcription factor *Hif1a* deletion were exposed to ALI induced by mechanical ventilation. Succinate metabolism was assessed in alveolar-epithelial via mass spectrometry as well as redox measurements and evaluation of lung injury. In WT mice, ALI induced by mechanical ventilation decreased SDHA activity and increased succinate in alveolar-epithelial. In vitro, cell-permeable succinate decreased epithelial inflammation during stretch injury. Mice with inducible alveolar-epithelial *Sdha* deletion ($Sdha^{loxp/loxp}$ SPC-CreER mice) revealed reduced lung inflammation, improved alveolar barrier function, and attenuated histologic injury. Consistent with a functional role of succinate to stabilize HIF, $Sdha^{loxp/loxp}$ SPC-CreER experienced enhanced Hif1a levels during hypoxia or ALI. Conversely, $Hif1a^{loxp/loxp}$ SPC-CreER showed increased inflammation with ALI induced by mechanical ventilation. Finally, wild-type mice treated with intratracheal dimethlysuccinate were protected during ALI. These data suggest that targeting alveolar-epithelial SDHA dampens ALI via succinate-mediated stabilization

Abbreviations: ALI, acute lung injury; ARDS, acute respiratory distress syndrome; AT II cells, alveolar-epithelial type 2 cells; BAL, bronchoalveolar lavage; BALF, bronchoalveolar lavage fluid; HIF, hypoxia-inducible factor; SDHA, succinate dehydrogenase A; TCA cycle, tricarboxylic acid cycle; WT, wild type.

Christine U. Vohwinkel and Ethan J. Coit are contributed equally to this work.

R01DK109574; HHS | NIH | National Heart, Lung, and Blood Institute (NHLBI), Grant/Award Number: R01HL154720; DOD | Defense Advanced Research Projects Agency (DARPA), Grant/Award Number: W81XWH2110032

of HIF1A. Translational extensions of our studies implicate succinate treatment in attenuating alveolar inflammation in patients suffering from ARDS.

KEYWORDS

ALI, alveolar epithelium, ARDS, HIF, inflammation, mechanical ventilation, SDHA, succinate

1 | INTRODUCTION

Acute lung injury (ALI) is an inflammatory lung disease caused by injurious stimuli or acute infections to the lung, typically resulting in symptoms of severe pulmonary edema and uncontrolled lung inflammation.[1] ALI manifests itself as acute respiratory distress syndrome (ARDS) in patients,[2,3] representing a severe threat to critically ill patients both in morbidity and in mortality with an overall mortality of 40%, and significant long-term disabilities in ARDS survivors.[4-8] Alveolar-epithelial type II (ATII) cells are susceptible to injurious insults that can lead to ALI, and the extent of alveolar-epithelial injury determines the severity of ARDS.[9,10] Therapy for ARDS is mainly supportive, and critically ill patients often require mechanical ventilation to support their lung function and maintain sufficient oxygen levels, with mechanical ventilation causing further injury to the alveolar epithelium. Other causes of ARDS—such as infection with coronavirus SARS-CoV2—primarily target alveolar-epithelial cells and can cause ARDS by causing alveolar inflammation and cell death.[11] Therefore, novel therapeutic approaches targeting alveolar-epithelial injury and hyperinflammation during ARDS are areas of intense research.[12-15]

Recent studies are providing evidence that carbohydrate metabolites and intermediates, in addition to their canonical function as energy substrate, play key functions in regulating inflammatory endpoints and can resolve lung inflammation.[16-19] Furthermore, hypoxia-inducible transcription factor HIF1A is a critical regulator of alveolar-epithelial carbohydrate metabolism during ALI.[20] Historically, HIF was identified in the 1990s as the transcription factor responsible for regulating hypoxia-elicited increases in erythropoietin and other hypoxia-dependent gene products.[21,22] Importantly, laboratory studies of ALI showed that during in vitro or in vivo models of alveolar injury, HIF1A is stabilized and contributes to optimal alveolar-epithelial carbohydrate metabolism.[20] These studies point out that HIF1A is stabilized by succinate. Previous studies from the field of oncology provide evidence that succinate can function as a pharmacologic activator of HIF.[23-25] However, the role of alveolar-epithelial succinate dehydrogenase (SDH) and its implications on succinate metabolism and HIF-elicited lung protection are largely unknown.

SDH is a unique metabolic enzyme since it plays a functional role in both the tricarboxylic acid (TCA) cycle and during mitochondrial respiration. In the TCA cycle, SDH is responsible for the oxidation of succinate to fumarate, and thereby directly controls intracellular levels of its upstream metabolite succinate.[26-28] In addition, it functions in oxidative phosphorylation as complex II of the electron transport chain.[28] Due to its role in the TCA cycle, SDH is critical for controlling intracellular succinate levels. Succinate is the upstream metabolite of SDH and is therefore directly under the control of SDH. SDH has four distinct subunits, SDHA-SDHD, with SDHA carrying the critical enzymatic activity that is responsible for the conversion of succinate to fumarate.[28,29] In order to study in the functional roles of alveolar-epithelial succinate metabolism during ALI, we generated a novel transgenic mouse model with targeted deletion of *Sdha* specifically in AT II cells. Our studies demonstrate that mice with ATII-specific *Sdha* deletion succinate levels in their alveolar epithelia are elevated and mice are protected from ALI induced by mechanical ventilation. Extension of these studies revealed that $Sdha^{loxp/loxp}$ SPC-CreER mice had increased Hif1a levels during ALI, which likely contributes to the observed protection during lung injury caused by mechanical ventilation. In line with those findings, mice with deletion of *Hif1a* in alveolar epithelial cells of the lungs ($Hif1a^{loxp/loxp}$ SPC-CreER mice) experience more severe lung injury. Finally, pharmacologic studies with cell-soluble succinate attenuated lung inflammation and histologic tissue injury during ALI in vivo.

2 | MATERIALS AND METHODS

2.1 | Cell culture and treatment

A549 cells (American Type Culture Collection (ATTC), Manassas/VA, USA (ATCC Cat# CRM-CCL-185, RRID:CVCL_0023) and primary alveolar epithelial type 2 cells (AT II cells) were cultured as described previously[30,31] in Dulbecco's modified Eagle medium (DMEM) with 4.5 g/L glucose and stable L-glutamine, 10% fetal bovine serum (FBS), and 1% penicillin/streptomycin mix (all from Corning Cellgro, Manassas/VA, USA). Cells were incubated in a humidified atmosphere of 5% CO_2/95% air at 37°C.

2.2 | Lentiviral generation of cell lines with knockdown of SDHA

A cell line with stable decreased expression of SDHA was generated by lentiviral-mediated shRNA expression as described previously.[20] To summarize: pLKO.1 lentiviral vector (Sigma-Aldrich, targeting SDHA had the shRNA sequence of CCG GGCATCTGCTAAAGTTTCAGATCTCGAGATCTG AAACTTTAGCAGAT GCTTTTT (TRCN0000028093). For controls, non-targeting control shRNA (SHC001: Sigma, St Louis/MO, USA, (RRID: Addgene_8453)) was used. Lentiviral suspensions carrying the plasmid were produced at the Functional Genomics Core Facility of the University of Colorado Boulder. The suspension was used for infection of A549 cells, and cells were selected with puromycin (1 μg/mL) for at least two passages before initiating stretch experiments.

2.3 | In vitro stretch model

In order to mimic cyclic mechanical stretch as it occurs during injurious mechanical ventilation, we utilized a previously described in vitro model that applies cyclic mechanical stretch to cultured pulmonary epithelial cells.[20] In short, cells were plated on BioFlex culture plates (FlexCell International, Burlington/ NC, USA) that were coated with collagen type1 and cells were allowed to attach. Pulmonary epithelial cells were grown to 80% confluence and seeded with a density of 3 million per well. All cells were cultured in 4 mL medium (DMEM, 4.5 g/L glucose, 10% FBS, 0.02% L-Glutamine). Plates were then placed on a FlexCell FX 4000T tension Plus System. Cells were stretched at 30% and a sine wave of 5s on, 5s off. Alveolar epithelial cells were then collected at specified time points and processed for further analysis. For controls, cells were cultured under identical conditions without application of cyclic mechanical stretch.

2.4 | Mice

Wild-type mice (BL6C57) were purchased from Jackson Laboratories (IMSR Cat# JAX:000664, RRID: IMSR_JAX:000664). Mice with Cre exclusively expressed in alveolar epithelial cells ($Sftpc^{tm1(cre/ERT2)Blh}$, JAX stock #028054, (IMSR Cat# JAX:028054, RRID: IMSR_JAX:028054)) were generously provided by Bridget Hogan (Duke University, Durham NC).[32] We opted for the $Sftpc^{tm1(cre/ERT2)Blh}$ system, due to reports of off-target toxicity in SPC-tet-O-Cre animals.[33] For tissue-specific knockout in the alveolar epithelium, Sdha floxed mice ($Sdha^{tm2a}$(KOMP)*Wtsi*) obtained from UC Davis were crossbred with a flippase expressing mouse line (FLPe, Ozgen Bentley/WA, Australia, (IMSR Cat# JAX:016226, RRID: IMSR_JAX:016226)) to remove the neomycin cassette and generate homozygous $Sdha^{loxp/loxp}$ mice. $Sdha^{loxp/loxp}$ mice were crossed with SPC-CreER animals to generate animals with ATII-specific *Sdha* suppression (Figure 3A). Conditional knockout was induced by 75 mg/kg/d i.p. tamoxifen over 5 days as described.[34] Genotyping of the resulting $Sdha^{loxp/loxp}$ SPC-CreER mice was performed via PCR on tails to determine Cre and loxp expression as well as ensure specific deletion of the floxed area of *Sdha* by testing for null PCR (GeneTyper, New York/NY, USA). SPC-CreER animals were used as control animals in studies addressing the tissue-specific *Sdha,* respectively, *Hif1a* knockout mice. Controls were matched for sex (male or female mice), weight (weighing 18-25g), and age (between 10 and 12 weeks) at the time of harvest for all genotypes.

2.5 | Murine model of ALI

Mice were ventilated for 4 hours at low or high inspiratory pressure levels to investigate the effect of alveolar epithelial *Sdha* or *Hif1a* deletion during ALI, as described previously.[8] A peak inspiratory pressure (PIP) of 45 cm H_2O was used for inducing ALI in mice, and a PIP of 15 cm H_2O served as the control condition. Animals were anesthetized with pentobarbital [70 mg/kg intraperitoneally (i.p.) for induction and 20 mg/kg per hour for maintenance] and were maintained at a stable body temperature by a warming table, using a rectal thermometer probe in a closed-loop circuit. A tracheotomy was performed, and the tracheal tube was connected to a mechanical ventilator (Siemens Servo 900C and Draeger Evita 2 Dura, with pediatric tubing). Mice were ventilated with 100% inspired oxygen.

2.6 | Ambient hypoxia exposure

Mice were maintained in normobaric normoxia or hypoxia for 24 hours. For hypoxia, mice were placed into a hypobaric chamber at a simulated altitude of 18 000 ft above sea level (395 Torr), conditions equivalent to 10% atmospheric oxygen. Normoxic mice remained in Denver (5, 280 ft) ambient air.

2.7 | Isolation of murine alveolar-epithelial cells

Primary alveolar epithelia were isolated from 10- to 12-week-old male or female mice matched in age, sex, and weight as described previously.[35,36] Mice were deeply anesthetized with intraperitoneal pentobarbital (70 mg/kg). Mice were exsanguinated by removing the left atrium, and lungs were then lavaged with sterile PBS via the right ventricle.

Dispase (Corning Lifesciences, Tewksbury, MA, USA) was subsequently instilled intra-tracheally followed by a low-melting point agarose plug. Lungs were removed intact and incubated for 45 minutes at room temperature. Tissue was teased apart manually and then passed through a 70-micron cell strainer (BD Bioscience, Franklin Lakes /NJ, USA). The cell mixture was then labeled with a mixture of CD16/32, TER119, CD45, and CD90 (all from BD Bioscience) and subsequently incubated with streptavidin-labeled magnetic beads for negative selection for alveolar-epithelial cells. In the final step, fibroblasts were removed by adherence to a petri dish for 2 hours.

2.8 | Immunoblotting

For Western immunoblotting, cells were washed twice with ice-cold PBS and lysed with 1x cell lysis buffer (Cell Signaling Technology, Danvers/ MA, USA) including protease inhibitor PMSF (effective concentration 100 µg/mL). For immunoblotting of HIF1A, we extracted the nuclear protein fraction from alveolar-epithelial cells using a commercially available kit according to the manufacturer's instructions (Thermo Fisher Scientific, Waltham/MA, USA). Protein concentrations were determined using QuickStart Bradford dye reagent (Bio-Rad Laboratories Inc, Hercules / CA, USA), and equal protein amounts were denatured in sample buffer, separated by SDS-electrophoresis, transferred to nitrocellulose membrane, blocked in 5% skim-milk [w/v] in TBS incl. 1% Tween-20 [v/v], and probed with the respective primary antibodies: HIF1A (Novus Biologicals, Centennial /CO, USA, clone H1alpha67, Novus Cat. # NB100-105, RRID: AB_10001154), SDHA (Abcam, Cambridge, UK, ab137040 RRID: AB_2884996 (prelim)) and b-actin (Sigma-Aldrich Cat. # A5441, RRID: AB_476744). Secondary antibodies were as follows: HRP anti-rabbit and (both from Cell Signalling Technology: Cat. #7074, RRID: AB_2099233 and Cat. # 7076, RRID: AB_330924). Densitometry was performed with ImageJ (NIH).

2.9 | Histopathological evaluation of acute lung injury

Lungs were explanted and prepared for paraffin embedding as described.[8] 5-µm sections were stained with H&E. Assessment of histological lung injury was performed as described previously[37] by grading using the following categories: a) infiltration or aggregation of inflammatory cells in air space or vessel wall: 1, only wall; 2, few cells (one to five cells) in air space; 3, intermediate; and 4, severe (air space congested); b) interstitial congestion and hyaline membrane formation: 1, normal lung; 2, moderate (<25% of lung section); 3, intermediate (25%-50% of lung section); and 4, severe (>50% of lung section); and c) hemorrhage: 0, absent; 1, present. Six representative images were obtained from each animal and were analyzed independently by 2 investigators, blinded to group assignments.

2.10 | Transmission electron microscopy (TEM)

Lung tissue was harvested immediately after euthanasia, cut into small pieces (3 mm^3), and fixed by immersion in 2% glutaraldehyde at 4°C, rinsed in 0.1 M phosphate buffer (pH 7.4), followed by postfixation in 1% osmium tetroxide, and block staining in 1% aqueous uranyl acetate, dehydrated using alcohol. The tissues were embedded in 100 EPON for 48 hours at 70°C. Ultra-thin sections of 70 nm were cut and stained 2% uranyl acetate and lead citrate, and examined under a JEOL JEM-1400Plus (JEOL USA Peabody, MA) transmission electron microscope. Representative images were obtained from each animal and were analyzed blinded to group assignments.

2.11 | Sample collection and measurement of BALF protein content

Bronchoalveolar lavage fluid (BALF) was obtained by lavaging the lungs 3 times with 1 mL PBS. After centrifugation at 300 g for 5 minutes at 4°C, cell-free BAL was immediately snap-frozen for subsequent studies. Pulmonary tissue was flushed with 10 mL saline via the right ventricle, and either snap-frozen in liquid nitrogen and stored at −80°C or conserved in formalin for histologic analysis. Protein content of BALF was measured via Bradford Assay as described previously.[38]

2.12 | Transcriptional analysis (qPCR)

Total RNA was isolated from primary ATII cells, A549 cells, or murine lung tissue using Qiagen RNeasy Mini Kit by following the manufacturer's protocol, and c-DNA was generated using iScript cDNA Synthesis Kit (Bio-Rad Laboratories Inc). RNA transcript levels were determined by real-time PCR (iCycler, Bio-Rad Laboratories Inc). Primers were obtained from Quantitect (Qiagen, Hilgen, Germany). The following primers were used for transcriptional analysis: Mm: β-Actin—QT01136772, IL-6—QT00098875, CXCL-1—QT100115647, Irg-1—QT00250166, Sdha—QT00265237, Sdhb—QT00150206, Sdhc—QT00157108, Sdhd—QT01037582. Hs: β-Actin—QT01680476 (housekeeping gene), IL-6—QT00083720, IL-8—QT00006822, IRG-1—QT01530424. The expression of Sod2, Cat, Gpx1, HO-1, and Prdx-1genes in whole lung samples was assessed by qRT-PCR using the primers as described before[39] as follows:

qPCRSOD2For (5′-CTGGACAAACCTGAGCCCTA-′3), qPCRSOD2Rev (5′-TGATAGCCTCCAGCAACTCTC-′3), qPCRCATFor (5′-CAGCGACCAGATGAAGCA-′3), qPCRCATRev (5′-CTCCGGTGGTCAGGACAT-′3), qPCRGPx1For (5′-ACAGTCCACCGTGTATGCCTTC-′3), qPCRGPx1Rev(5′-CTCTTCATTCTTGCCATTCTCCTG-′3), qPCRHO-1For (5′-GGTCAGGTGTCCAGAG-AAGG-′3), qPCRHO-1Rev (5′-CTTCCAGGGCCGTGTAGATA-′3), qPCRPRDX1For (5′-GTGAGACCTGTGGCTCGAC-′3), qPCRPRDX1Rev (5′-TGTCCATCTGGCATAACAGC-′3).

2.13 | Metabolite analysis

Alveolar-epithelial cells freshly isolated from the lungs of mice using antibody selection were used for metabolomics analysis. Metabolites from frozen cell pellets were extracted using ice-cold methanol/acetonitrile/water (5:3:2) at a ratio of 2×10^6 cells per mL by vortexing for 30 minutes at 4 degrees C. Samples were clarified through centrifugation (10 min at 10 000 rpm, 4 degrees C), and 10 µL of supernatant was analyzed using a 5 minutes C18 gradient on a Thermo Vanquish UHPLC coupled online to a Thermo Q Exactive mass spectrometer operating in positive and negative ion modes (separate runs) as previously described in detail.[40] Samples were normalized to cell count.

2.14 | ATP measurement

ATP Bioluminescence Assay Kit CLS II (Roche, Basel, Switzerland) was used to measure the ATP from whole lung samples. A POLARstar Omega luminometer (BMG LabTech Inc Cary/ NC, USA) was used to measure relative luminescence of the samples according to manufacturer guidelines. The measured concentration of ATP was normalized to the protein concentration of the samples, which were measured using Bradford Assay.

2.15 | Mitochondrial ROS analysis with electron paramagnetic resonance (EPR)

Mitochondrial ROS in lung tissue were measured by EPR as previously described[41] with several modifications. Freshly harvested lung tissue was weighed and homogenized in 300 µL sucrose using the BEAD RUPTOR (Omni International, Kennesaw, GA). The tissue homogenate was immediately placed on ice and homogenate transferred to a 1.5-mL Eppendorf tube. 30 µL homogenate was added to 166 µL KHB + 100 µM DTPA (metal chelators), treated with 4 µL of the mitochondrial specific spin probe, mito-TEMPO-H (9.5 mM stock, final concentration 0.2 mM), and incubated for 1h at 37°C. After 1h, 150 µL was loaded into Teflon tubing and flash frozen in liquid nitrogen. EPR measurements were done at 77k using the Bruker EMXnano X-band spectrometer (Bruker, San Jose, CA). EPR acquisition parameters were microwave frequency = 9.65 GHz; center field = 3438 G; modulation amplitude = 6.0 G; sweep width = 150 G; microwave power = 0.316 mW; total number of scans = 2; sweep time = 60 seconds; and time constant = 1.28 ms Nitroxide radical concentration was obtained by double integration followed by Spin Count module (Bruker) and expressed as the nitroxide radical, and the concentration was normalized sample protein concentrations measured by Bradford Assay.

2.16 | Antioxidant enzyme analysis

Superoxide dismutase (SOD) and catalase are enzymes that catalyze the breakdown of oxygen radicals**.** For measuring superoxide dismutase (SOD), or catalase activity, the following assays were used, respectively: Lung tissues were homogenized in 0.5 mL of cold PBS in a TissueLyser II (QIAGEN) for 2 minutes at 30 Hz, and the supernatant separated by centrifugation at 5000 rpm for 5 minutes at 4C. Aliquots of the same extract were used for measuring the enzymatic activities. SOD activity was measured using the cytochrome c reduction inhibition assay as described previously.[42] Crude extract samples were added to a mix of 50 mM xanthine, 10 mM cytochrome c, and 0.1 mM EDTA in 50 mM phosphate buffer pH 7.8. The sample-reaction mix was homogenized and the rate of change of absorbance at 550-526 nm monitored with a diode array spectrophotometer at 25 degrees °C. When the rate of change was unnoticeable, 4 mU/mL of xanthine oxidase (XO) was added and the changes in absorbance recorded. The rates of change in the cytochrome c reduction were between 30% and 70% of the control rate of the reaction mix plus XO without sample. The rate values were used to quantify superoxide dismutase with a SOD software program (developed by Joe M. McCord). Catalase activity was assessed according to Bergmeyer et al[43] using fresh stock concentrations of H_2O_2. Samples of the crude extracts or concentrated supernatants were added to 20 mM H_2O_2 in 50 mM potassium phosphate pH 7.0 and incubated at 25°C, recording the changes at 240 nm. The catalase content was estimated using the 43.6 M-1 extinction coefficient. The protein content of crude extracts was measured using the method described by Lowry et al[44] Lipid peroxidation was assessed utilizing thiobarbituric acid reactive substances (TBARS).TBARS were measured using the method described by Ohkawa et al.[45]

2.17 | Statistical analysis

As primary outcomes, we assessed the severity of ALI by determining mRNA expression levels of pro-inflammatory

cytokines, pulmonary barrier function, measuring protein content in the bronchoalveolar lavage fluid (BALF), and histology. For analysis of metabolomics from ATII cells, each data point was isolated from a different animal. For cell line experiments, each experiment was carried out independently. For analysis of histology, two investigators, who were blinded to genotype and treatment, performed scoring independently. All statistical analyses were carried out using GraphPad Prism 8.1.2 (GraphPad Software, San Diego, CA, USA). We conducted Grubbs' tests on all eligible data to examine outliers. No outliers were identified. We conducted Shapiro-Wilk tests and constructed boxplots to examine normal distributions. All data approximately followed normal distributions and were summarized as means ± SD. Equal variances were evaluated by *F* test. Unless otherwise noted, we used the two-sample *t* tests to compare means when equal variances were satisfactory. In data with significantly different variances, Welch's *t* tests were used. Bonferroni adjustment was employed in experiments involving more than one comparison. We reported two-sided *P* values, and *P* values less than .05 were considered statistically significant. Statistical analysis of the data was reviewed by a faculty-level statistician. The authors had full access to the data and have read and agree to the manuscript as written.

3 | RESULTS

3.1 | ALI induced by mechanical ventilation decreases activity of SDHA in alveolar epithelia

While ALI and associated mechanical ventilation carry a significant morbidity and mortality, many episodes of ALI are self-limited, suggesting the presence of endogenous protective pathways.[19,20,46-50] Previous studies had suggested that inhibition of SDHA could lead to the accumulation of succinate and stimulation of endogenous protective pathways via enhancing the stabilization of HIF1A.[20] Based on these studies, we further investigated functional roles of alveolar SDHA during lung injury. To induce ALI in mice in vivo, we exposed mice to mechanical ventilation using pressure-controlled ventilation (Figure 1A).[8,51] For this purpose, wild-type (WT) mice matched in age, gender, and weight underwent tracheostomy and were mechanically ventilated over 4 hours at an inspiratory pressure level of 45 cm H_2O. Subsequently, we isolated AT II cells and analyzed SDH-dependent metabolites (Figure S1). We found that TCA cycle metabolites up- and downstream of SDH were altered in their abundance, including increased levels of succinate (upstream of SDH) and decreased levels of fumarate (downstream of SDH) as shown in Figure 1B,C. These measurements indicate that ALI induced by mechanical ventilation is associated with decreased SDHA activity (Figure 1D). In order to discern the mechanism of SDHA inhibition, we first examined the transcription levels of all SDH subunits in ATII cells and found no difference in their individual transcript levels in response to ALI (Figure 1E), indicating that the observed reduction in activity of SDHA activity is not transcriptionally regulated.

Previous studies had indicated that the immune responsive gene 1 (*Irg-1*) protein, also known as *cis*-aconitate decarboxylase, catalyzes the production of itaconate from the TCA cycle intermediate *cis*-aconitate (see Figure S1). Itaconate has been shown to act as a competitive inhibitor of SDHA, leading to an accumulation of succinate.[52,53] Therefore, we tested whether *Irg-1* is involved in SDHA inhibition in alveolar epithelia during ALI. These studies revealed that *Irg-1* mRNA expression was significantly induced in the whole lungs of mice exposed to ALI (Figure 1F), and itaconate levels were elevated in isolated AT II cells of mice exposed to ALI induced by mechanical ventilation (Figure 1G). Taken together, these studies suggest that during ALI, SDHA activity is decreased, which likely is mediated by increased inhibition through itaconate.

3.2 | Succinate attenuates epithelial inflammation during cyclic mechanical stretch exposure

After having shown that during ALI, SDHA activity is decreased and concomitantly alveolar succinate levels are elevated in vivo, we next pursued in vitro studies to examine the functional implications of elevated succinate levels on inflammatory responses. For this purpose, we utilized an in vitro model of epithelial injury that mimics injurious mechanical ventilation.[54] Alveolar-epithelial cells are plated on a mechanical device that exposes them to cyclic mechanical stretch, and thereby causes injury to alveolar-epithelial cells, and concomitant increases in inflammation. Based on previous studies,[20] we hypothesized that the inhibition of SDHA and subsequent accumulation of succinate in alveolar epithelia functions to dampen inflammation. In these studies, we exposed the human pulmonary epithelial cell line A549 to injurious stretch conditions (30% stretch over 24h), following pre-treatment with permeable succinate (dimethlysuccinate) or vehicle control. Dimethlysuccinate treatment was associated with decreased inflammatory responses when pulmonary epithelia were exposed to cyclic mechanical stretch for 24 hours, as shown by significantly decreased mRNA expression of the pro-inflammatory cytokine *Il-6* and chemokine *Il-8 c*ompared with controls (Figure 2B,C). To further examine the functional consequences of SDHA inhibition on epithelial inflammation, we subsequently generated A549 cells with stable shRNA-mediated knock down of *Sdha* (Figure 2D). Subsequent exposure of pulmonary epithelia

(A)

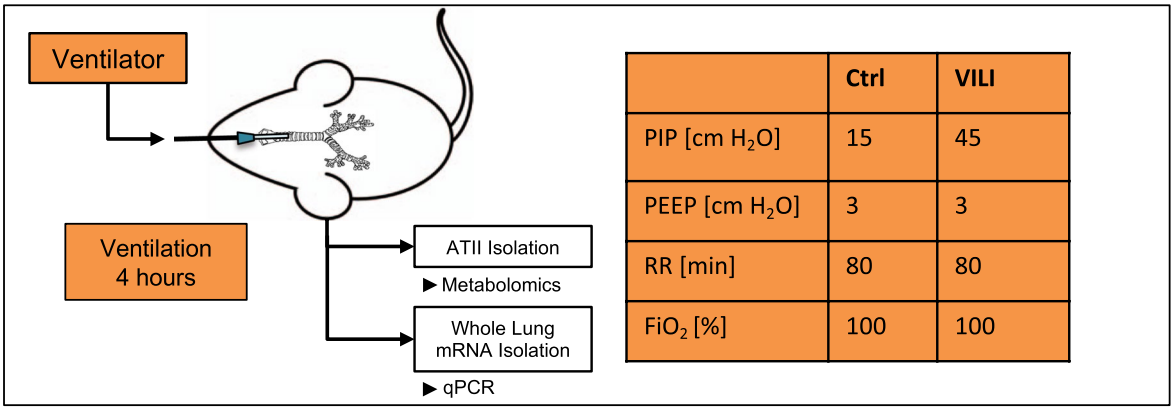

	Ctrl	VILI
PIP [cm H_2O]	15	45
PEEP [cm H_2O]	3	3
RR [min]	80	80
FiO_2 [%]	100	100

PIP15 PIP 45

(B)

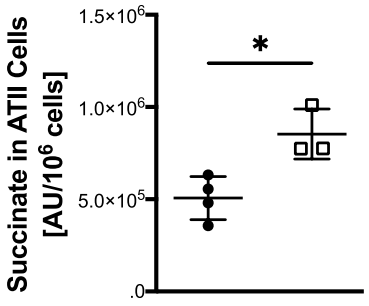

(C)

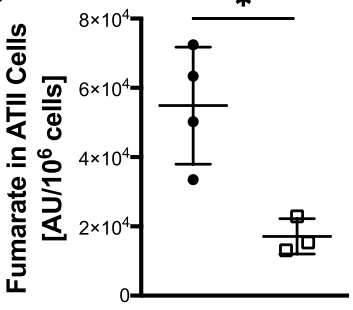

(D)

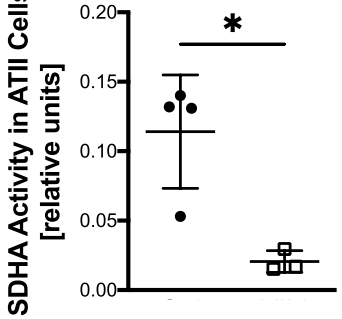

(E)

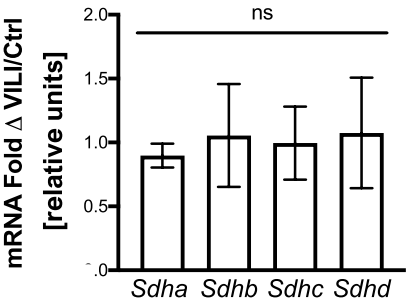

(F)

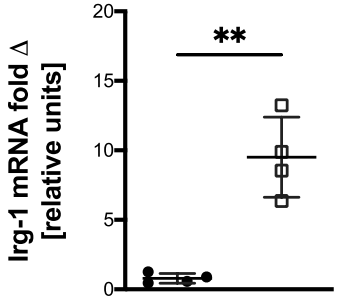

(G)

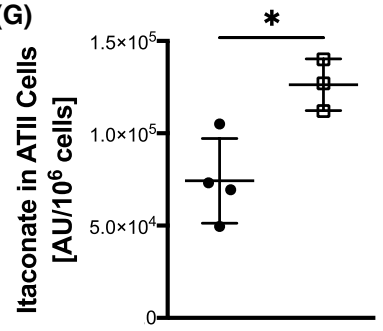

FIGURE 1 ALI induced by mechanical ventilation is associated with reduced activity of SDHA in alveolar epithelium. A, Schematic overview of ventilation experiments: 10- to 12-week-old mice were anesthetized and ventilated for 4 h with the following parameters: Pressure-controlled ventilation (PCV), peak inspiratory pressure (PIP) 15 cm H_2O in the control group and 45 cm H_2O in the experimental group, PEEP 3 cm H_2O, respiratory rate 80/min, and FiO_2 1.0 were set equally in both groups. B and C, TCA cycle intermediates succinate and fumarate were determined with mass spectroscopy in ATII cells after mice were exposed to 15 or 45 cm H_2O PIP. D, Succinate dehydrogenase (SDHA) activity was determined by calculating the succinate to fumarate ratio. mRNA expression of SDH subunits (E) and Irg-1(F) was determined with qPCR. (G) Itaconate abundance was measured in ATII cells via mass spectroscopy. Data are represented as mean ± SD, n = 3-4, ns-not significant, **P* <.05, ***P* <.01, Welch's *t* test in F, t = 5.993 and *df* = 3.09; two-sample *t* test in G, t = 3.43 and *df* = 5. A total of 21 animals were used

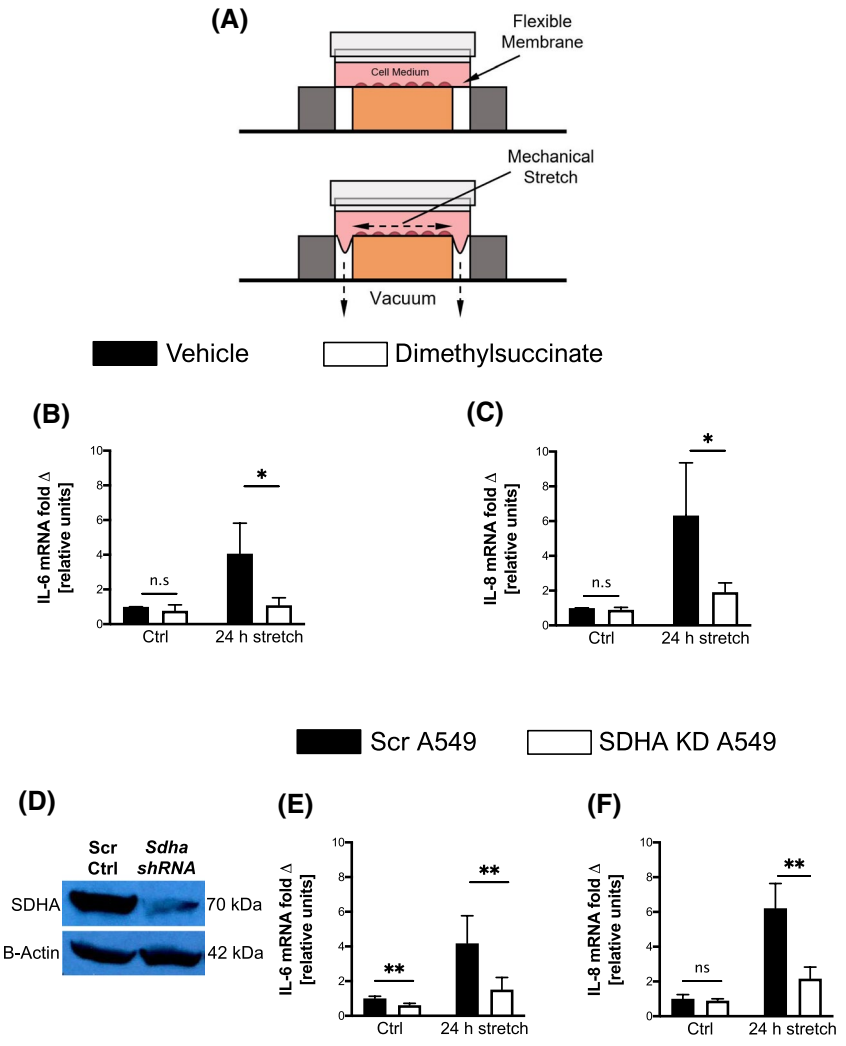

FIGURE 2 Succinate attenuates epithelial inflammation during cyclic mechanical stretch exposure. A, Schematic of in vitro cyclic mechanical stretch system. Cells were plated on a flexible membrane coated with collagen and vacuum to induce mechanical stretch to simulate injurious ventilation in vitro. B and C, mRNA expression of pro-inflammatory cytokine IL-6 and chemokine IL-8 was determined in human alveolar-epithelial cell line A549 with qPCR after 24 h of mechanical stretch and treatment with cell-permeable 10 μM dimethlysuccinate or vehicle. D, Western blot confirmation of SDHA knockdown in A549 cells *SDHA* shRNA, control cells were transfected with scrambled shRNA (scrRNA). E and F, mRNA expression of IL-6 and. IL-8 in A549 cells with stable knockdown of *SDHA* (shRNA *SDHA*) or scrambled controls (Scr A549). Cells were exposed to 24 h of cyclic mechanical stretch or control conditions. Data are represented as mean ± SD, n = 5-6, ***P* <.01, ***P* <.001; Welch's *t* test with Bonferroni adjustment

with shRNA-mediated knockdown of SDHA to cyclic mechanical stretch over 24 hours demonstrated significantly attenuated increases in the expression of pro-inflammatory cytokine IL-6 and chemokine IL-8 (Figure 2E,F), as compared to controls. Taken together, these studies indicate that pharmacologic-mediated increases in succinate or genetic repression of SDH is associated with decreased inflammation of pulmonary epithelial cells exposed to cyclic mechanical stretch such as occurs during injurious mechanical ventilation.

3.3 | Generation and characterization of mice with alveolar-epithelial deletion of *Sdha*

Based on the above in vitro studies indicating a protective role of succinate mediated by SDHA inhibition on epithelial inflammation during stretch, we next set out to perform a more detailed examination of the functional role of alveolar-epithelial SDHA by generating transgenic mice with a conditional deletion of *Sdha* in ATII cells ($Sdha^{loxp/loxp}$ SPC-CreER) (Figure 3A). This approach is critical, since germ-line deletion

of *Sdha* is associated with embryonic lethality.[55] *Sdha*$^{loxp/loxp}$ SPC-CreER animals grow to adulthood without any congenital malformations and reach a weight similar to SPC-CreER control animals (Figure 3B). To characterize functional consequences of alveolar *Sdha* deletion on TCA cycle metabolites, we next measured TCA cycle intermediates upstream from SDHA (α-ketoglutarate and succinate, see Figure S1) using freshly isolated ATII cells from mice exposed to ALI

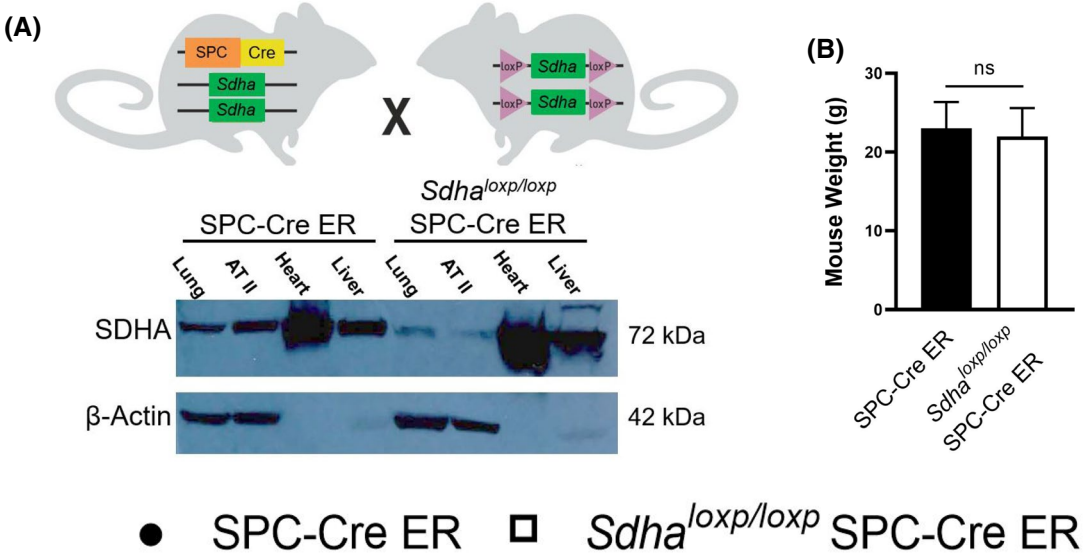

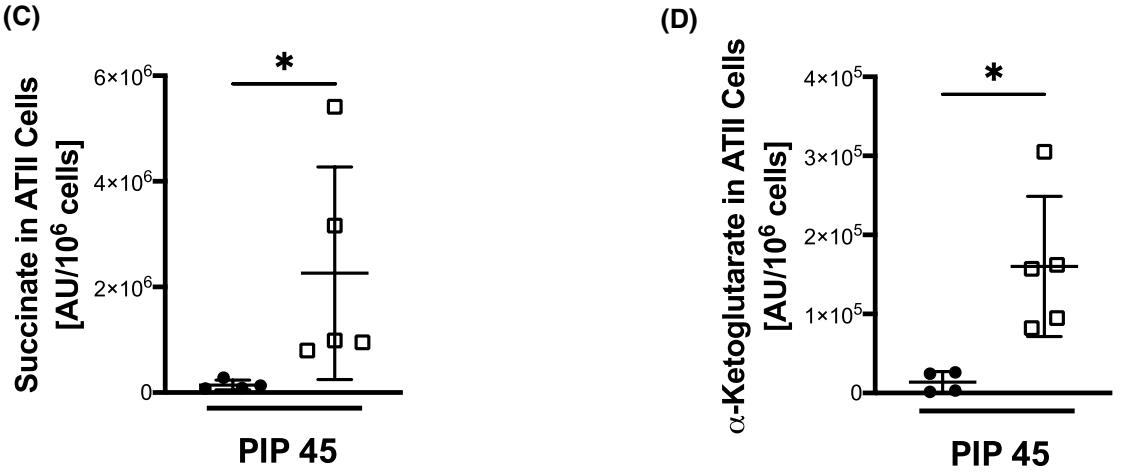

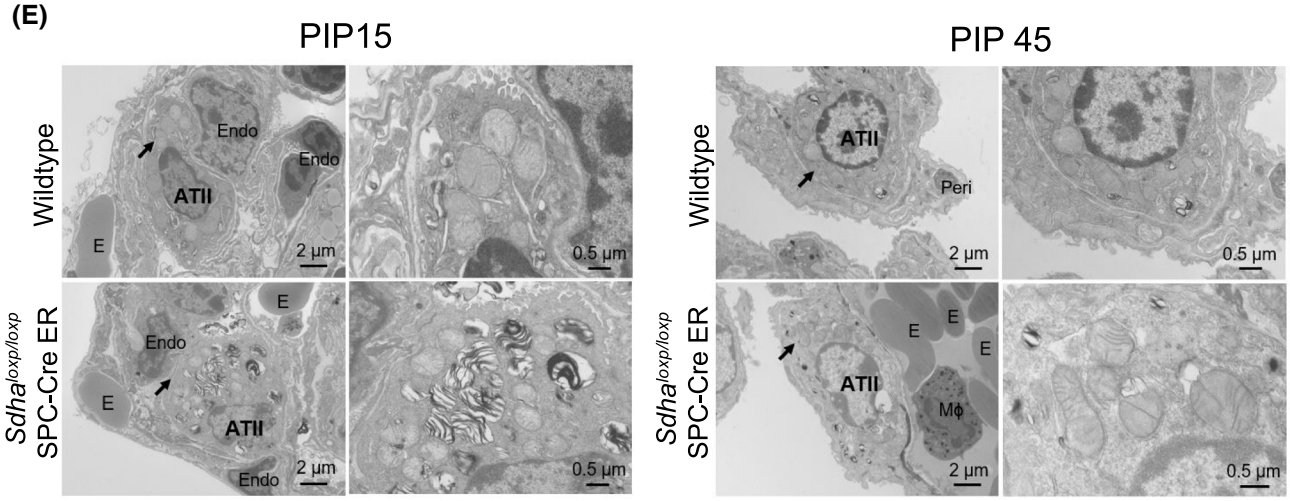

FIGURE 3 Generation and characterization of mice with alveolar epithelial deletion of *Sdha*. A, Generation of mice with AT II-specific deletion of *Sdha*. Animals homozygous for floxed *Sdha* allele ($Sdha^{loxp/loxp}$) were crossed with SPC-CreER mice to generate the $Sdha^{loxp/loxp}$ SPC-CreER line. Conditional Sdha suppression was induced by i.p. tamoxifen. Sdha suppression in AT II cells was confirmed with Western blot. B, Weights of $Sdha^{loxp/loxp}$ SPC-CreER mice compared with SPC-CreER control mice. Both groups were age matched at 10-12 weeks of age after having received tamoxifen for 5 days, 2 weeks prior to ventilation. C and D, Quantification of TCA cycle intermediates succinate (C) and α-ketoglutarate (D) in ATII cells after ventilation with 45 cm_2 H_2O by mass spectroscopy. E, Electron microscopic images of wild-type and $Sdha^{loxp/loxp}$ SPC-CreER animals in control (PIP 15 cm H_2O) and experimental (PIP 45 cm H_2O) conditions. ATII = alveolar epithelial type II, E = erythrocyte, Endo = endothelial cell, Mϕ = Macrophage, Peri = pericytes. Data are represented as mean ± SD, n = 4-5, $*P < .05$, B; Welch's *t* test in C, t = 2.97 and *df* = 4; Welch's *t* test in D, t = 3.64 and *df* = 4.22. Total of 17 animals were used for panels C-E (panel B encompasses animals from Figures 3-5)

(Figure 3C,D). Consistent with a functional defect of Sdha, alveolar epithelia isolated from $Sdha^{loxp/loxp}$ SPC-CreER had significantly higher levels of succinate or α-ketoglutarate than SPC-CreER control mice (Figure 3C,D). Since SDH could also play functional roles in mitochondrial respiration, we next characterized global mitochondrial function in $Sdha^{loxp/loxp}$ SPC-CreER mice or SPC-CreER control animals. Comparison of electron microscopic images by a blinded reviewer of freshly isolated lung tissue of SPC-CreER $Sdha^{loxp/loxp}$ mice or control animals showed no structural differences and appear normal (Figure 3E). In addition, measurement of the ATP concentration between SPC-CreER and SPC-CreER $Sdha^{loxp/loxp}$ and analysis of the activity of mitochondrial ROS production or important lung antioxidant enzymes showed no biologically relevant differences between both genotypes (Figure 4A-J), providing further evidence that SDHA function in alveolar epithelium is predominantly constrained to the TCA cycle. This contrasts with studies in endothelial cells, which linked shear stress induced endothelial pyroptosis to inhibition of SDH subunit B (SDH-B) and subsequent mitochondrial injury and increased ROS production.[56] However, as we did not find an effect of injurious ventilation on SDH-B (Figure 1E), this could explain while ROS production was not affected in the $Sdha^{loxp/loxp}$ SPC-CreER animals.

Taken together, these studies indicate that mice with ATII-specific deletion of SDHA have no structural mitochondrial abnormalities or respiratory chain dysfunction but increased succinate levels during ALI secondary to genetic *Sdha* deletion.

3.4 | Alveolar-epithelial *Sdha* deletion mediates lung protection during ALI

After having characterized mice with conditional deletion of *Sdha* in ATII cells, we next pursued functional studies of ALI induced by injurious mechanical ventilation. For the purpose of these studies, we exposed $Sdha^{loxp/loxp}$ SPC-CreER mice or SPC-CreER controls matched in sex, age, and weight to ALI. Both genotypes showed increased inflammation after 4 hours of injurious mechanical ventilation, compared to mice exposed to low-pressure mechanical ventilation as control. However, $Sdha^{loxp/loxp}$ SPC-CreER mice exposed to ALI experienced a marked attenuation of the inflammatory response compared with the SPC-CreER animals as evidenced by decreased expression of pro-inflammatory cytokine and chemokine transcript levels in ATII cells (Figure 5 A,B) and protein content of broncho-alveolar fluid (Figure 5C). Moreover, assessment of histologically visible lung damage by a blinded reviewer demonstrated attenuated injury (Figure 5D,E). In addition, we found no apparent evidence for sex-specific differences in lung inflammation between male or female $Sdha^{loxp/loxp}$ SPC-CreER mice (see Figure S2). Taken together, these studies provide genetic in vivo evidence for a protective role of alveolar-specific *Sdha* deletion and implicate succinate elevation in attenuating alveolar injury.

3.5 | Alveolar-epithelial Hif1a stabilization as mediator of succinate-elicited lung protection

After having shown that mice with conditional deletion of *Sdha* in ATII cells experience attenuated lung injury in the context of elevated succinate levels when exposed to mechanical ventilation, we subsequently pursued studies to address a potential mechanism. Previous studies had indicated that stabilization of HIF in cancers can involve the inhibition or mutation of SDH, leading to elevation of succinate levels.[25] These studies suggest that succinate can function as inhibitor of prolyl hydroxylases (PHDs)—a group of enzymes that target HIF for proteasomal degradation[57-60]—thereby causing normoxic HIF stabilization.[23,25,61] Other studies had provided genetic and pharmacologic in vivo evidence that HIF1A expressed in alveolar-epithelial cells provides lung protection during ALI.[20] Therefore, we pursued the hypothesis that deletion of *Sdha* is associated with elevated HIF1A levels as a mechanism for succinate-dependent lung protection. Since hypoxia is a strong stimulus for HIF1A stabilization,[62] we first set out to determine HIF1A stabilization in $Sdha^{loxp/loxp}$ SPC-CreER exposed to ambient hypoxia. These studies revealed increased Hif1a stabilization in $Sdha^{loxp/loxp}$ SPC-CreER compared with SPC-CreER control animals following 24 hours of exposure to 10% hypoxia (Figure 6A,B). Next, we explored Hif1a stabilization

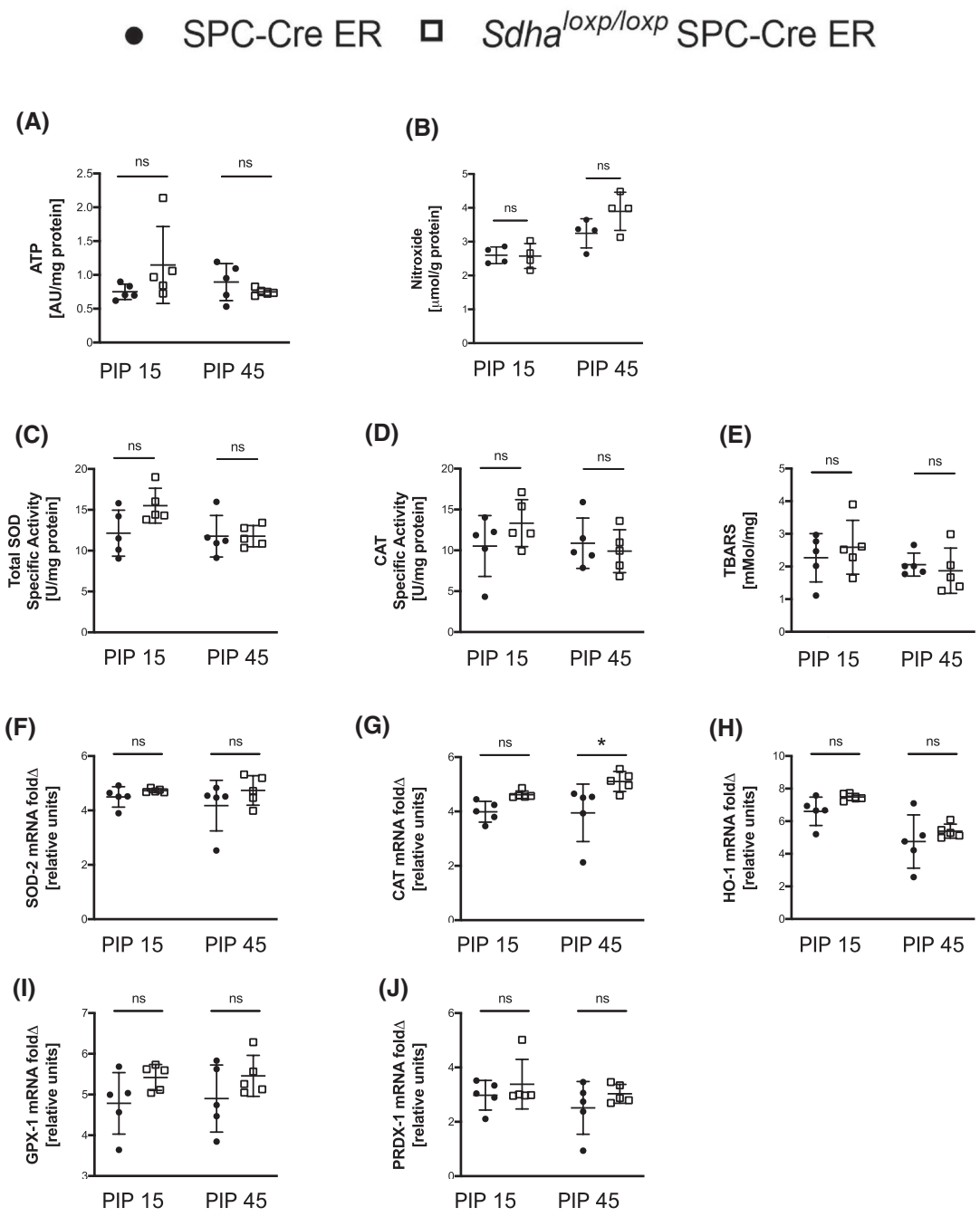

FIGURE 4 alveolar-epithelial *Sdha* deletion does not affect ATP generation or ROS production. A, ATP concentrations were measured with bioluminescence assay and normalized to protein concentration of whole lung samples. B-E, Concentration of mitochondrial ROS normalized to protein concentration of homogenized whole lung measured with EPR spin probes as nitroxide concentration (B) and enzyme activity of total superoxide dismutase- SOD (C), catalase-CAT (D), and TBARS-thiobarbituric acid reactive substances (E). F-J, mRNA expression of ROS enzymes: SOD-2 (F), CAT (G), HO-1-hem oxygenase 1 (H), GPX-1-gluthathione peroxidase1 (I), PRDX-1-peroxireducin 1 (J) from whole lung samples via qPCR. Data represented as mean ± SD, n = 4-5, ns-not significant, **P* <.05, two-sample *t* test or Welch's *t* test with Bonferroni adjustment. Total of 20 animals were used

in *Sdha*$^{loxp/loxp}$ SPC-CreER compared with SPC-CreER control animals after ALI induced by mechanical ventilation. These studies showed that *Sdha*$^{loxp/loxp}$ SPC-CreER mice display increased Hif1a stabilization compared with SPC-CreER (see Figure S3A). To further investigate the functional role of Hif1a in ALI induced by mechanical ventilation, we next generated mice with conditional deletion of *Hif1a* (*Hif1a*$^{loxp/loxp}$ SPC-CreER) by crossing surfactant Cre + mice (SPC-CreER) with *Hif1a*$^{loxp/loxp}$ mice (Figure 6C,D). *Hif1a*$^{loxp/loxp}$ SPC-CreER animals grow to adulthood without any congenital malformations

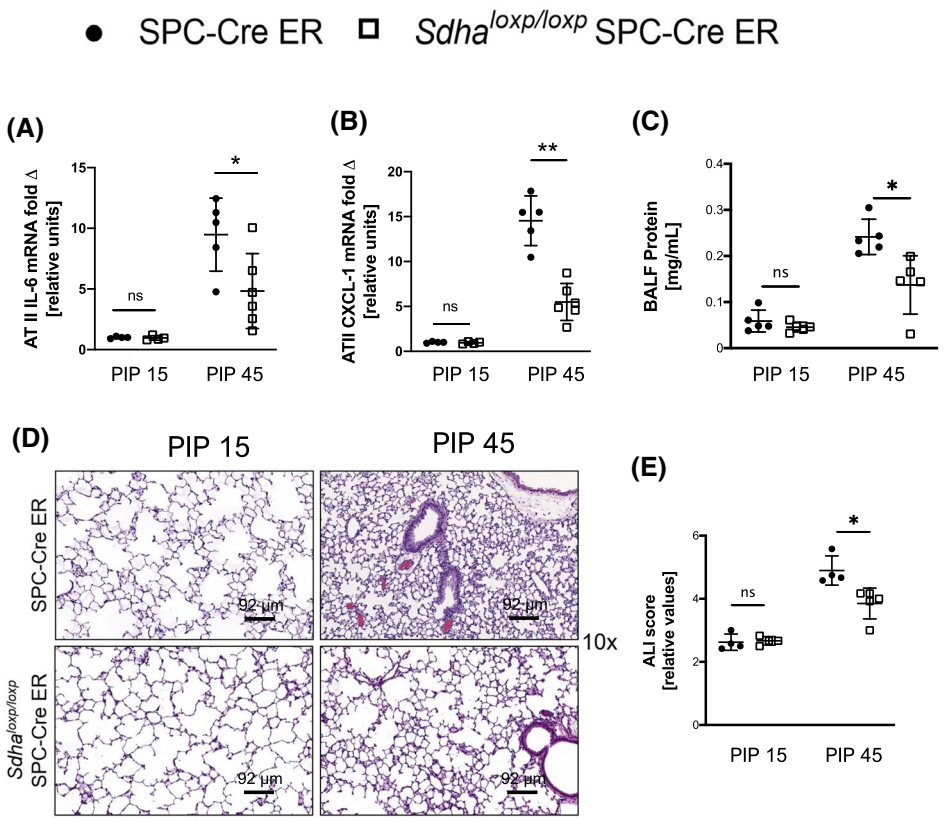

FIGURE 5 Tissue-specific alveolar-epithelial *Sdha* deletion mediates lung protection during ALI: A-E, *Sdha*$^{loxp/loxp}$ SPC-CreER mice or age, gender, and weight-matched controls (SPC-CreER) were exposed PIP of 45 cm H_2O to induce lung injury or control ventilation (15 cm H_2O). A and B, mRNA expression was determined from ATII cells with qPCR. C, Protein concentration was measured in bronchoalveolar lavage fluid (BALF). D, Representative images of H&E-stained lungs from mice subjected to PIP of 15 vs 45 cm H_2O. E, Cumulative lung injury score which is a combined score of cellular infiltrates, interstitial congestion and hyaline membrane formation, and hemorrhage. Data are represented as mean ± SD, n = 4-7, ns-not significant, **P* <.05, ***P* <.01. Welch's *t* test with Bonferroni adjustment. Total of 35 animals were used

and reach a weight similar to SPC-CreER control animals (Figure 6E). However, *Hif1a*$^{loxp/loxp}$ SPC-CreER when exposed to ALI induced by mechanical ventilation experienced exacerbated lung injury compared with control SPC-CreER mice, evidenced by elevated transcript levels of pro-inflammatory cytokine IL-6 (Figure 6F) and chemokine CXCL-1 (Figure 6G) in whole lung tissue and leakage of albumin into the bronchoalveolar fluid (Figure 6H). Consequently, lung injury assessed by histologic ALI score in *Hif1a*$^{loxp/loxp}$ SPC-CreER animals showed exacerbated lung injury compared with SPC-CreER group (Figure 6I,J). These findings in our mice with improved target-specific Cre expression in the SPC-CreER mice[63] are consistent with previous studies in mice epithelial deletion of *Hif1a*$^{loxp/loxp}$ SPC.[20] HIF1-mediated effects have been shown to be sex-specific.[64] However, we found no differences in CXCL-1 chemokine expression between male and female animals in response to ALI (see Supplemental Figure 3B). Taken together, these findings provide indirect evidence that *Sdha* deletion and concomitant elevation of alveolar succinate levels can provide lung protection through increased HIF1A levels and enhanced "hypoxia signaling" during ALI.

3.6 | Local delivery of dimethlysuccinate attenuate inflammation in lung injury induced by mechanical ventilation

Based on our observations that SPC-CreER *Sdha*$^{loxp/loxp}$ animals do have increased succinate levels in their alveolar epithelia and show robust protection during ALI induced by mechanical ventilation, we next set out to test whether we could recapitulate the protective effects of alveolar-epithelial *Sdha* deletion via therapeutic succinate supplementation. To achieve delivery to alveolar epithelia, we chose to give dimethlysuccinate (cell-permeable form of succinate) via intratracheal route (i.t.). In these studies, we pre-treated mice with dimethlysuccinate (10 µM, 50 µL i.t.) 15 minutes prior to induction of ALI (Figure 7A), with the control groups receiving equal volumes of vehicle (0.9% NaCl). Consistent with our previous studies, treatment with dimethlysuccinate was associated with decreased expression of the transcript levels of in IL-6 and CXCL-1 during ALI induced by mechanical ventilation (Figure 7B,C). Conversely, lung

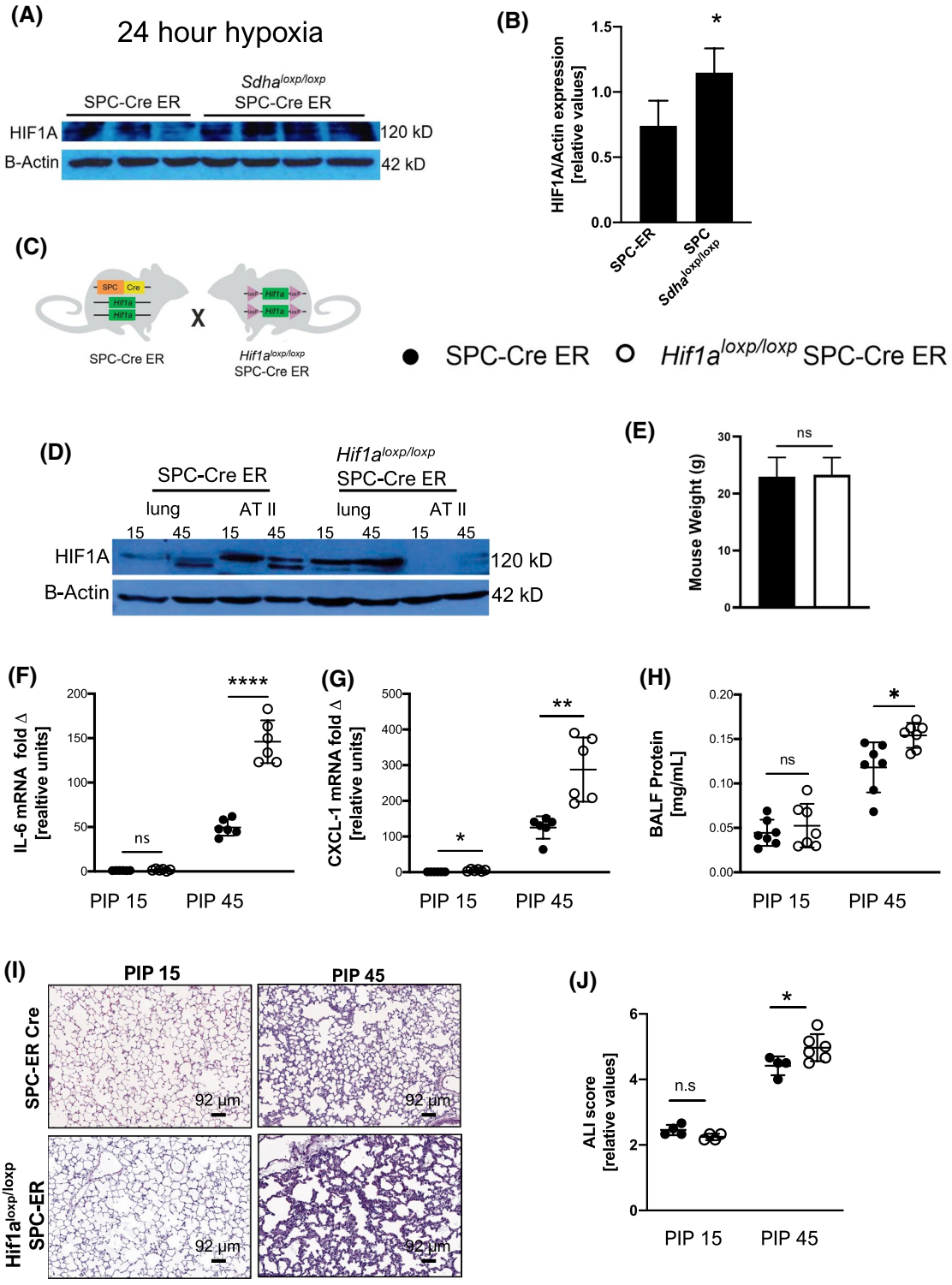

FIGURE 6 Alveolar-epithelial Hif1a stabilization as mediator of succinate-elicited lung protection. A and B, ATII cells were isolated from SPC-CreER and *Sdha*$^{loxp/loxp}$ SPC-CreER mice exposed to 24 h of hypoxia (10% FiO_2). ATII cells were lysed, and nuclear Hif1a expression was determined with Western blot and quantified. C, Generation of mice with AT II-specific deletion of *Hif1a*. Animals homozygous for floxed *Hif1a* allele (*Hif1a*$^{loxp/loxp}$) were crossed with SPC-CreER mice to generate the *Hif1a*$^{loxp/loxp}$ SPC-CreER $^{loxp/loxp}$ line. Conditional Hif1a suppression was induced by i.p. tamoxifen. D, Confirmation of Hif1a suppression in ATII cells with Western blot. E, Weights of *Hif1a* $^{loxp/loxp}$ SPC-CreER mice compared with SPC-CreER control mice. F and G, mRNA expression was determined from whole lung tissue with qPCR after mice were subjected to injurious (PIP 45 cm H_2O) or control ventilation (PIP 15 cm H_2O). H, Protein concentration was measured in BALF. I, Representative images of H&E-stained lungs from mice subjected to PIP 15 cm H_2O) vs PIP 45 cm H_2O). J, Cumulative lung injury score which is a combined score of cellular infiltrates, interstitial congestion and hyaline membrane formation, and hemorrhage. Data are represented as mean ± SD, n = 3-7, ns-not significant, **P* <.05, ***P* <.01, *****P* <.0001, B and E, two-sample *t* test; F-G, unpaired, Welch's *t* test with Bonferroni adjustment. Total of 47 animals were used

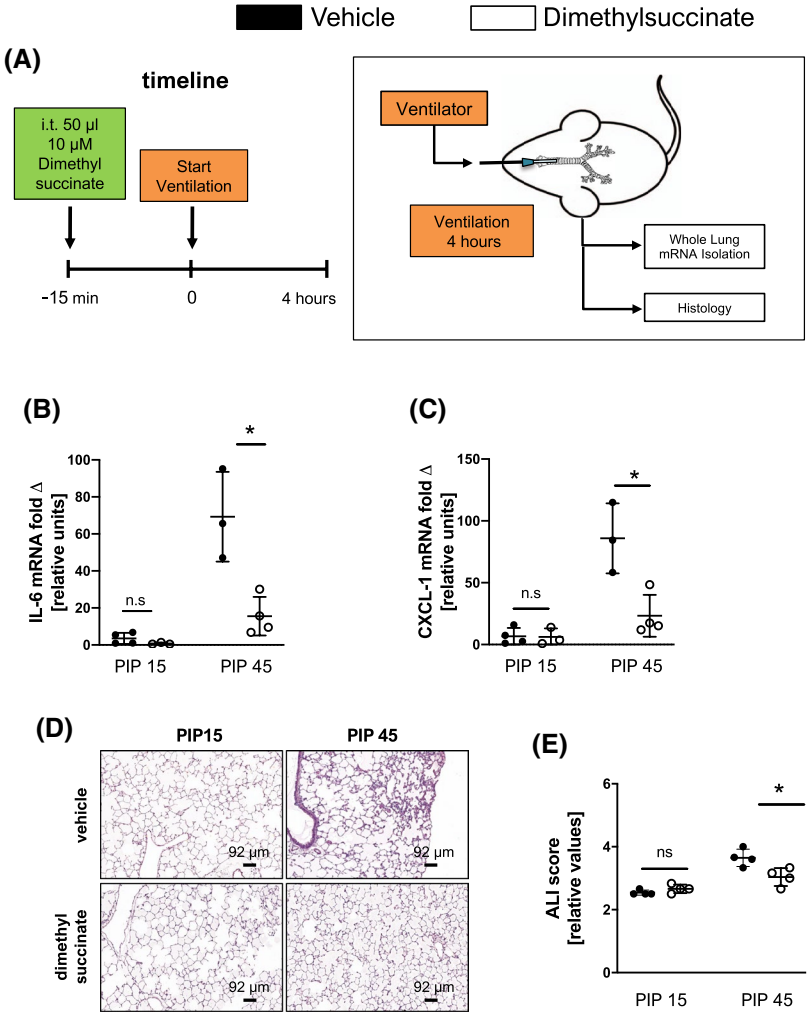

FIGURE 7 Local delivery of dimethylsuccinate attenuates inflammation in ALI. A. Schematic overview of the experiments. Anesthetized mice received either 50 µL of vehicle (physiol. NaCl) or 10 µM dimethyl succinate i.t. 15 min prior to initiation of control (PIP 15) or injurious ventilation PIP 45); after 4 h, lungs were removed. B and C, mRNA expression was determined from whole lung tissue with qPCR after mice were subjected to ventilation with PIP 15 vs 45 cm H_2O. D, Representative images of H&E-stained lungs from mice subjected to PIP 15 vs 45 cm H_2O. E, Cumulative lung injury score which is a combined score of cellular infiltrates, interstitial congestion and hyaline membrane formation, and hemorrhage. Data are represented as mean ± SD, n = 3-4, ns-not significant, $*P < .05$, Welch's *t* test with Bonferroni adjustment. Total of 30 animals were used, and no animal was excluded from analysis

injury assessed by histologic ALI scoring showed attenuated lung injury in animals treated with dimethlysuccinate compared with control animals (Figure 7 D,E). Taken together, those studies indicate that local, i.t. treatment with dimethlysuccinate functions to dampen inflammation during ALI.

4 | DISCUSSION

The present studies were designed to gain additional insight on the impact of carbohydrate metabolites as regulators of alveolar inflammation during ARDS. Previous studies had suggested a central role of the TCA intermediate succinate as endogenous regulator of alveolar-epithelial hypoxia signaling.[20] Since SDHA represents the central regulator for cellular succinate generation, we pursued pharmacologic and genetic in vivo studies to address the functional role of alveolar succinate metabolism during ARDS. These studies demonstrated that mice with alveolar-epithelial SDHA deletion ($Sdha^{loxp/loxp}$ SPC-CreER mice) experience higher succinate levels and concomitant lung protection during murine models of ARDS. For example, $Sdha^{loxp/loxp}$ SPC-CreER mice experienced attenuated lung inflammation, less pulmonary edema, and improved histologic lung injury scores when exposed to injurious mechanical ventilation. Studies to address the mechanism of succinate-mediated lung protection showed that alveolar Hif1a levels were elevated in $Sdha^{loxp/loxp}$ SPC-CreER mice during hypoxia or during exposure to ARDS. Indeed, mice with alveolar-epithelial *Hif1a* deletion ($Hif1a^{loxp/loxp}$ SPC-CreER) showed exacerbated lung injury during exposure to ARDS. Finally, studies exploring the SDHA pathway therapeutically revealed that pharmacologic treatment with intra-tracheal succinate was associated with improved outcomes during ARDS induced by mechanical ventilation. Interestingly, i.t delivery of succinate appeared to improve that ALI phenotype more than alveolar-epithelial-specific deletion of *Sdha* as the wild-type mice treated with i.t. succinate had better ALI scores than the $Sdha^{loxp/loxp}$ SPC-CreER mice, which is suggestive of extra-epithelial effects of succinate. Succinate mediates HIF1A stabilization by preventing its proteasomal degradation by PHDs. Although we cannot exclude that exogenous succinate might have non–HIF1A-mediated protective effects, we do not expect succinate, if

given to *Hif1a*$^{loxp/loxp}$ SPC-CreER mice, to have a significant protective effect in contrast to the wild-type animals. Beside the alveolar epithelium, the pulmonary endothelium is also a critical part of the pulmonary barrier.[65] Succinate has been shown to affect endothelial VEGF and ROS production,[56,66] and therefore, increased alveolar-epithelial succinate could have a secondary effect on the endothelium. Taken together, these studies indicate a protective role of alveolar-epithelial succinate and suggest pharmacologic approaches to elevate alveolar-epithelial succinate levels in ARDS treatment.

The current studies suggest that alveolar-epithelial succinate can function to protect during ARDS by enhancing HIF1A levels as a mechanism of lung protection. Several previous studies have suggested a protective role of HIF during ARDS. Some of these studies looked at pulmonary immune responses during hyperoxia.[67] Landmark research from the laboratory of Dr Sitkovsky had shown that mice exposed to poly-microbial sepsis as a model of ARDS experience different disease outcomes dependent on the level of oxygenation they are exposed to. Mice kept at lower oxygen concentrations had improved outcomes, as compared to mice kept at 100% oxygen. The authors link those differences in outcomes to attenuated levels of HIF and dampened signaling events through the A2A adenosine receptor when exposed to 100% oxygen,[68] thereby providing indirect evidence for a protective role of HIF1A during ARDS.[69] Subsequent studies linked those findings to a functional role of natural killer T cells.[70] Extracellular adenosine has been shown to function as a protective regulator of alveolar inflammation during ARDS[13,14,47] and can signal through 4 distinct adenosine receptors (A1, A2A, A2B, and A3).[49] In addition to the A2A adenosine receptor, previous studies had identified a functional role of HIF1A in regulating the A2B adenosine receptor during ARDS.[71] Functional studies of A2B signaling during ARDS models had shown a critical role of the A2B adenosine receptor in improving alveolar fluid clearance, and attenuating lung injury induced by mechanical ventilation,[72] or during LPS-induced lung injury.[73] Again, other studies have suggested that HIF can function to provide lung protection during ARDS by optimizing alveolar-epithelial carbohydrate metabolism.[20,74] During injurious conditions, alveolar epithelia are exquisitely dependent on the glycolytic utilization of carbohydrates as metabolic source. HIF is a known key regulator of the glycolytic system. In line with those findings, mice with alveolar-epithelial *Hif1a* deletion fail to elevate their glycolytic flux rates.[20] Other investigators were able to confirm a lung-protective role of HIF-signaling in different models of ARDS,[74-76] including studies of virus-associated ARDS.[77] Taken together with the current genetic and pharmacologic studies, these findings implicate HIF activation as a pharmacologic strategy to dampen lung injury during ARDS. Interestingly, ongoing clinical trials are currently evaluating the impact of HIF activators in ARDS prevention or treatment in COVID-19 patients (ClinicalTrials.gov Identifier: NCT04478071).

The functional role of succinate as a stabilizer of HIF1A has been suggested in previous studies from the cancer field.[23-25] The critical step in regulating the stability of HIF1A involves PHD-mediated targeting of the alpha-subunit of HIF for proteasomal degradation. Inhibition of PHDs can occur due to lack of oxygen, thereby accounting for hypoxia-mediated HIF stabilization.[21,78] Similarly, several small molecules have been identified as PHD inhibitors, which also accounts for the ability of cellular succinate to function as HIF activator. The current studies highlight an anti-inflammatory role of HIF activation in alveolar-epithelial cells. In contrast, different functional outcomes have been shown for succinate in endothelial cells mediated the activating G protein–coupled receptor 91[79] or in inflammatory cells of the myeloid lineage. For example, studies in macrophages exposed to LPS identified succinate as a metabolite in innate immune signaling, which enhances interleukin-1β production during inflammation.[80] Similarly, upon LPS stimulation, macrophages shift from producing ATP by oxidative phosphorylation to glycolysis while also increasing succinate levels.[81] Furthermore, recent studies show that plasma succinate is elevated in patients with ARDS secondary to trauma, which is in line with an animal of hemorrhagic shock-induced ALI.[66,82] Additionally, pulmonary neutrophils could be primed with succinate, so that they responded to a second stimulus (LPS) with an increased inflammatory response.[82] These findings elucidate the complex nature of succinate-mediated immune signaling in the context of ALI depending on the mechanism (trauma vs injurious ventilation) and primary target cell (alveolar epithelium vs myeloid cell). Taken together with the current findings, these studies suggest cell-specific roles of succinate signaling in mediating inflammatory endpoints. However, the combination of attenuating alveolar inflammation while simultaneously enhancing myeloid inflammatory responses[12] is likely highly beneficial for ARDS treatment, where attenuating alveolar inflammation can function to dampen pulmonary edema and improving alveolar-capillary function, while simultaneously allowing myeloid cells to function in pathogen elimination.[83]

In summary, the present studies highlight a novel role for alveolar-epithelial succinate signaling in lung protection during ARDS. In extension of the present findings, several therapeutic implications for ARDS treatment can be considered for translation from bench to bedside. These approaches include direct use of cell-permeable forms of succinate, inhibition of SDHA as a means for elevating intracellular succinate levels, or the use of pharmacologic HIF activators. The later have been used successfully in the form of orally available HIF activators for the treatment or renal anemia.[84,85] Repurposing HIF activators for ARDS prevention or treatment could represent a novel therapeutic approach, which is urgently needed for conventional ARDS,

or for the treatment of patients experiencing COVID-19–associated ARDS.[1,67]

ACKNOWLEDGMENTS

National Institute of Health Grants R01DK122796, R01DK109574, R01HL133900, R01HL154720, and Department of Defense Grant W81XWH2110032 to HKE, National Institute of Health Grant K12HD068372, K08HL130586 and Parker B. Francis Fellowship to CUV. We thank Eric Wartchow from Department of Pathology, Colorado Children's Hospital, for technical assistance with the electron microscopy and Dr Angelo D'Alessandro and Dr Ryan Fredericks (University of Colorado, School of Medicine) for their help with the mass spectroscopy experiments. The authors thank Dr Yangyu Wang from University of Texas Health Science Center for her help with data organization and Dr Xu Zhang from University of Texas Health Science Center for excellent advice in regard to statistical analysis.

CONFLICTS OF INTEREST

The authors declare no competing interests.

AUTHOR CONTRIBUTIONS

C.U. Vohwinkel, R.M. Tuder, and H.K. Eltzschig designed the research studies. C.U. Vohwinkel, E.J. Coit, N. Burns, H. Elajaili, D. Hernandez-Saavedra conducted the experiments. C.U. Vohwinkel, E.J. Coit, and X. Yuan analyzed the data. T. Eckle provided knockout animals. C.U. Vohwinkel, E.J. Coit, R.M. Tuder, E. Nozik, and H.K. Eltzschig wrote the manuscript.

ETHICS

All experimental protocols were approved by the Institutional Review Board of the University of Colorado, Anschutz Medical Campus. Animal experiments were approved by the local Institutional Animal Care and Use Committee [protocol numbers B104917(04)1E and 00128]. They were in accordance with the US Law on the Protection of Animals and the National Institutes of Health Guidelines for use of live animals.

ORCID

Christine U. Vohwinkel https://orcid.org/0000-0001-8959-157X

REFERENCES

1. Williams GW, Berg NK, Reskallah A, Yuan X, Eltzschig HK. Acute respiratory distress syndrome. *Anesthesiology*. 2021;134(2):270-282.
2. Ranieri VM, Rubenfeld GD, Thompson BT, et al. Acute respiratory distress syndrome: the Berlin Definition. *JAMA*. 2012;307:2526-2533.
3. Eltzschig HK, Carmeliet P. Hypoxia and inflammation. *N Engl J Med*. 2011;364:656-665.
4. Rubenfeld GD, Caldwell E, Peabody E, et al. Incidence and outcomes of acute lung injury. *N Engl J Med*. 2005;353:1685-1693.
5. Villar J, Blanco J, Anon JM, et al. The ALIEN study: incidence and outcome of acute respiratory distress syndrome in the era of lung protective ventilation. *Intensive Care Med*. 2011;37:1932-1941.
6. Herridge MS, Tansey CM, Matte A, et al. Functional disability 5 years after acute respiratory distress syndrome. *N Engl J Med*. 2011;364:1293-1304.
7. Mamary AJ, Kondapaneni S, Vance GB, Gaughan JP, Martin UJ, Criner GJ. Survival in patients receiving prolonged ventilation: factors that influence outcome. *Clin Med Insights Circ Respir Pulm Med*. 2011;5:17-26.
8. Hoegl S, Burns N, Angulo M, et al. Capturing the multifactorial nature of ARDS - "Two-hit" approach to model murine acute lung injury. *Physiol Rep*. 2018;6:e13648.
9. Montaner JS, Tsang J, Evans KG, et al. Alveolar epithelial damage. A critical difference between high pressure and oleic acid-induced low pressure pulmonary edema. *J Clin Invest*. 1986;77:1786-1796.
10. Wiener-Kronish JP, Albertine KH, Matthay MA. Differential responses of the endothelial and epithelial barriers of the lung in sheep to Escherichia coli endotoxin. *J Clin Invest*. 1991;88:864-875.
11. Tay MZ, Poh CM, Renia L, MacAry PA, Ng LFP. The trinity of COVID-19: immunity, inflammation and intervention. *Nat Rev Immunol*. 2020;20(6):363–374.
12. Neudecker V, Brodsky KS, Clambey ET, et al. Neutrophil transfer of miR-223 to lung epithelial cells dampens acute lung injury in mice. *Sci Transl Med* 2017;9(408):eaah5360.
13. Hoegl S, Brodsky KS, Blackburn MR, Karmouty-Quintana H, Zwissler B, Eltzschig HK. Alveolar epithelial A2B adenosine receptors in pulmonary protection during acute lung injury. *J Immunol*. 2015;195:1815-1824.
14. Eckle T, Hughes K, Ehrentraut H, et al. Crosstalk between the equilibrative nucleoside transporter ENT2 and alveolar Adora2b adenosine receptors dampens acute lung injury. *FASEB J*. 2013;27:3078-3089.
15. Gudernatsch V, Stefanczyk SA, Mirakaj V. Novel resolution mediators of severe systemic inflammation. *Immunotargets Ther*. 2020;9:31-41.
16. Antonioli L, Blandizzi C, Pacher P, Hasko G. Immunity, inflammation and cancer: a leading role for adenosine. *Nat Rev Cancer*. 2013;13:842-857.
17. Eltzschig HK, Sitkovsky MV, Robson SC. Purinergic signaling during inflammation. *N Engl J Med*. 2012;367:2322-2333.
18. Idzko M, Ferrari D, Eltzschig HK. Nucleotide signalling during inflammation. *Nature*. 2014;509:310-317.
19. Serhan CN, Chiang N, Dalli J, Levy BD. Lipid mediators in the resolution of inflammation. *Cold Spring Harb Perspect Biol*. 2014;7:a016311.
20. Eckle T, Brodsky K, Bonney M, et al. HIF1A reduces acute lung injury by optimizing carbohydrate metabolism in the alveolar epithelium. *PLoS Biol*. 2013;11:e1001665.
21. Yuan X, Lee JW, Bowser JL, Neudecker V, Sridhar S, Eltzschig HK. Targeting hypoxia signaling for perioperative organ injury. *Anesth Analg*. 2018;126(1):308-321.
22. Bowser JL, Lee JW, Yuan X, Eltzschig HK. The hypoxia-adenosine link during inflammation. *J Appl Physiol*. 2017;123:1303-1320.
23. Koivunen P, Hirsila M, Remes AM, Hassinen IE, Kivirikko KI, Myllyharju J. Inhibition of hypoxia-inducible factor (HIF) hydroxylases by citric acid cycle intermediates: possible links

between cell metabolism and stabilization of HIF. *J Biol Chem*. 2007;282:4524-4532.

24. MacKenzie ED, Selak MA, Tennant DA, et al. Cell-permeating alpha-ketoglutarate derivatives alleviate pseudohypoxia in succinate dehydrogenase-deficient cells. *Mol Cell Biol*. 2007;27:3282-3289.
25. Selak MA, Armour SM, MacKenzie ED, et al. Succinate links TCA cycle dysfunction to oncogenesis by inhibiting HIF-alpha prolyl hydroxylase. *Cancer Cell*. 2005;7:77-85.
26. Cordes T, Wallace M, Michelucci A, et al. Immunoresponsive Gene 1 and Itaconate Inhibit Succinate Dehydrogenase to Modulate Intracellular Succinate Levels. *J Biol Chem*. 2016;291:14274-14284.
27. Murphy MP, O'Neill LAJ. Krebs cycle reimagined: the emerging roles of succinate and itaconate as signal transducers. *Cell*. 2018;174:780-784.
28. Rutter J, Winge DR, Schiffman JD. Succinate dehydrogenase—assembly, regulation and role in human disease. *Mitochondrion*. 2010;10:393-401.
29. Rasheed M, Tarjan G. Succinate dehydrogenase complex: an updated review. *Arch Pathol Lab Med*. 2018;142:1564-1570.
30. Hoffman O, Burns N, Vadasz I, Eltzschig HK, Edwards MG, Vohwinkel CU. Detrimental ELAVL-1/HuR-dependent GSK3beta mRNA stabilization impairs resolution in acute respiratory distress syndrome. *PLoS One*. 2017;12:e0172116.
31. Vohwinkel CU, Buchackert Y, Al-Tamari HM, et al. Restoration of megalin-mediated clearance of alveolar protein as a novel therapeutic approach for acute lung injury. *Am J Respir Cell Mol Biol*. 2017;57:589-602.
32. Rock JR, Barkauskas CE, Cronce MJ, et al. Multiple stromal populations contribute to pulmonary fibrosis without evidence for epithelial to mesenchymal transition. *Proc Natl Acad Sci U S A*. 2011;108:E1475-E1483.
33. Rawlins EL, Perl AK. The a"MAZE"ing world of lung-specific transgenic mice. *Am J Respir Cell Mol Biol*. 2012;46:269-282.
34. Madisen L, Zwingman TA, Sunkin SM, et al. A robust and high-throughput Cre reporting and characterization system for the whole mouse brain. *Nat Neurosci*. 2010;13:133-140.
35. Beck JM, Preston AM, Wilcoxen SE, Morris SB, Sturrock A, Paine R 3rd. Critical roles of inflammation and apoptosis in improved survival in a model of hyperoxia-induced acute lung injury in Pneumocystis murina-infected mice. *Infect Immun*. 2009;77:1053-1060.
36. Mercer PF, Johns RH, Scotton CJ, et al. Pulmonary epithelium is a prominent source of proteinase-activated receptor-1-inducible CCL2 in pulmonary fibrosis. *Am J Respir Crit Care Med*. 2009;179:414-425.
37. Ehrentraut H, Clambey ET, McNamee EN, et al. CD73+ regulatory T cells contribute to adenosine-mediated resolution of acute lung injury. *FASEB J*. 2013;27:2207-2219.
38. Maeda M, Ozaki T, Yasuoka S, Ogura T. Role of alveolar macrophages and neutrophils in the defense system against infection of Pseudomonas aeruginosa in the respiratory tract and the effect of derivative of muramyl dipeptide. *Nihon Kyobu Shikkan Gakkai Zasshi*. 1990;28:135-142.
39. Hernandez-Saavedra D, Swain K, Tuder R, Petersen SV, Nozik-Grayck E. Redox regulation of the superoxide dismutases SOD3 and SOD2 in the pulmonary circulation. *Adv Exp Med Biol*. 2017;967:57-70.
40. Nemkov T, Reisz JA, Gehrke S, Hansen KC, D'Alessandro A. High-throughput metabolomics: isocratic and gradient mass spectrometry-based methods. *Methods Mol Biol*. 2019;1978:13-26.
41. Elajaili HB, Hernandez-Lagunas L, Ranguelova K, Dikalov S, Nozik-Grayck E. Use of electron paramagnetic resonance in biological samples at ambient temperature and 77 K. *J Vis Exp*. 2019;(143). https://doi.org/10.3791/58461
42. McCord JM, Fridovich I. Superoxide dismutase. An enzymic function for erythrocuprein (hemocuprein). *J Biol Chem*. 1969;244:6049-6055.
43. Bergmeyer HU. Measurement of catalase activity. *Biochem Z*. 1955;327:255-258.
44. Lowry OH, Rosebrough NJ, Farr AL, Randall RJ. Protein measurement with the Folin phenol reagent. *J Biol Chem*. 1951;193:265-275.
45. Ohkawa H, Ohishi N, Yagi K. Assay for lipid peroxides in animal tissues by thiobarbituric acid reaction. *Anal Biochem*. 1979;95:351-358.
46. Buckley CD, Gilroy DW, Serhan CN, Stockinger B, Tak PP. The resolution of inflammation. *Nat Rev Immunol*. 2013;13:59-66.
47. Eltzschig HK, Weissmuller T, Mager A, Eckle T. Nucleotide metabolism and cell-cell interactions. *Methods Mol Biol*. 2006;341:73-87.
48. Levy BD, Serhan CN. Resolution of acute inflammation in the lung. *Annu Rev Physiol*. 2014;76:467-492.
49. Poth JM, Brodsky K, Ehrentraut H, Grenz A, Eltzschig HK. Transcriptional control of adenosine signaling by hypoxia-inducible transcription factors during ischemic or inflammatory disease. *J Mol Med (Berl)*. 2013;91:183-193.
50. Serhan CN. Resolution phase of inflammation: novel endogenous anti-inflammatory and proresolving lipid mediators and pathways. *Annu Rev Immunol*. 2007;25:101-137.
51. Eckle T, Fullbier L, Grenz A, Eltzschig HK. Usefulness of pressure-controlled ventilation at high inspiratory pressures to induce acute lung injury in mice. *Am J Physiol Lung Cell Mol Physiol*. 2008;295:L718-L724.
52. Michelucci A, Cordes T, Ghelfi J, et al. Immune-responsive gene 1 protein links metabolism to immunity by catalyzing itaconic acid production. *Proc Natl Acad Sci U S A*. 2013;110:7820-7825.
53. Lampropoulou V, Sergushichev A, Bambouskova M, et al. Itaconate links inhibition of succinate dehydrogenase with macrophage metabolic remodeling and regulation of inflammation. *Cell Metab*. 2016;24:158-166.
54. Eckle T, Fullbier L, Wehrmann M, et al. Identification of ectonucleotidases CD39 and CD73 in innate protection during acute lung injury. *J Immunol*. 2007;178:8127-8137.
55. Dickinson ME, Flenniken AM, Ji X, et al. High-throughput discovery of novel developmental phenotypes. *Nature*. 2016;537:508-514.
56. Chen J, Zhang J, Wu J, et al. Low shear stress induced vascular endothelial cell pyroptosis by TET2/SDHB/ROS pathway. *Free Radic Biol Med*. 2020. https://doi.org/10.1016/j.freeradbiomed.2020.11.017
57. Kaelin WG Jr, Ratcliffe PJ. Oxygen sensing by metazoans: the central role of the HIF hydroxylase pathway. *Mol Cell*. 2008;30:393-402.
58. Kaelin WG. *Von Hippel-Lindau disease. Annu Rev Pathol*. 2007;2:145-173.
59. Kaelin WG. Proline hydroxylation and gene expression. *Annu Rev Biochem*. 2005;74:115-128.
60. Epstein AC, Gleadle JM, McNeill LA, et al. C. elegans EGL-9 and mammalian homologs define a family of dioxygenases that regulate HIF by prolyl hydroxylation. *Cell*. 2001;107:43-54.

61. Koivunen P, Lee S, Duncan CG, et al. Transformation by the (R)-enantiomer of 2-hydroxyglutarate linked to EGLN activation. *Nature*. 2012;483:484-488.
62. Lee JW, Ko J, Ju C, Eltzschig HK. Hypoxia signaling in human diseases and therapeutic targets. *Exp Mol Med*. 2019;51:1-13.
63. Gui YS, Wang L, Tian X, et al. SPC-Cre-ERT2 transgenic mouse for temporal gene deletion in alveolar epithelial cells. *PLoS One*. 2012;7:e46076.
64. Zhang Y, Dong X, Lingappan K. Role of HIF-1alpha-miR30a-Snai1 axis in neonatal hyperoxic lung injury. *Oxid Med Cell Longev*. 2019;2019:8327486.
65. Shah D, Torres C, Bhandari V. Adiponectin deficiency induces mitochondrial dysfunction and promotes endothelial activation and pulmonary vascular injury. *FASEB J*. 2019;33:13617-13631.
66. Li M, Li G, Yu B, Luo Y, Li Q. Activation of hypoxia-inducible factor-1alpha via succinate dehydrogenase pathway during acute lung injury induced by trauma/hemorrhagic shock. *Shock*. 2020;53:208-216.
67. Hanidziar D, Nakahori Y, Cahill LA, et al. Characterization of pulmonary immune responses to hyperoxia by high-dimensional mass cytometry analyses. *Sci Rep*. 2020;10:4677.
68. Ohta A, Sitkovsky M. Role of G-protein-coupled adenosine receptors in downregulation of inflammation and protection from tissue damage. *Nature*. 2001;414:916-920.
69. Thiel M, Chouker A, Ohta A, et al. Oxygenation inhibits the physiological tissue-protecting mechanism and thereby exacerbates acute inflammatory lung injury. *PLoS Biol*. 2005;3:e174.
70. Nowak-Machen M, Schmelzle M, Hanidziar D, et al. Pulmonary natural killer T cells play an essential role in mediating hyperoxic acute lung injury. *Am J Respir Cell Mol Biol*. 2013;48:601-609.
71. Eckle T, Kewley EM, Brodsky KS, et al. Identification of hypoxia-inducible factor HIF-1A as transcriptional regulator of the A2B adenosine receptor during acute lung injury. *J Immunol*. 2014;192:1249-1256.
72. Eckle T, Grenz A, Laucher S, Eltzschig HK. A2B adenosine receptor signaling attenuates acute lung injury by enhancing alveolar fluid clearance in mice. *J Clin Invest*. 2008;118:3301-3315.
73. Schingnitz U, Hartmann K, Macmanus CF, et al. Signaling through the A2B adenosine receptor dampens endotoxin-induced acute lung injury. *J Immunol*. 2010;184:5271-5279.
74. Tojo K, Tamada N, Nagamine Y, Yazawa T, Ota S, Goto T. Enhancement of glycolysis by inhibition of oxygen-sensing prolyl hydroxylases protects alveolar epithelial cells from acute lung injury. *FASEB J*. 2018;32:2258-2268.
75. McClendon J, Jansing NL, Redente EF, et al. Hypoxia-inducible factor 1alpha signaling promotes repair of the alveolar epithelium after acute lung injury. *Am J Pathol*. 2017;187:1772-1786.
76. Huang X, Zhang X, Zhao DX, et al. Endothelial hypoxia-inducible factor-1alpha is required for vascular repair and resolution of inflammatory lung injury through forkhead box protein M1. *Am J Pathol*. 2019;189:1664-1679.
77. Zhao C, Chen J, Cheng L, Xu K, Yang Y, Su X. Deficiency of HIF-1alpha enhances influenza A virus replication by promoting autophagy in alveolar type II epithelial cells. *Emerg Microbes Infect*. 2020;9:691-706.
78. Lee JW, Koeppen M, Seo SW, et al. Transcription-independent Induction of ERBB1 through hypoxia-inducible factor 2A provides cardioprotection during ischemia and reperfusion. *Anesthesiology*. 2020;132:763-780.
79. Li Y, Liu Y, Wang C, et al. Succinate induces synovial angiogenesis in rheumatoid arthritis through metabolic remodeling and HIF-1alpha/VEGF axis. *Free Radic Biol Med*. 2018;126:1-14.
80. Tannahill GM, Curtis AM, Adamik J, et al. Succinate is an inflammatory signal that induces IL-1beta through HIF-1alpha. *Nature*. 2013;496:238-242.
81. Mills EL, Kelly B, Logan A, et al. Succinate dehydrogenase supports metabolic repurposing of mitochondria to drive inflammatory macrophages. *Cell*. 2016;167(2):457-470.e13.
82. Nunns GR, Vigneshwar N, Kelher MR, et al. Succinate activation of SUCNR1 predisposes severely injured patients to neutrophil-mediated ARDS. *Ann Surg*. 2020. https://doi.org/10.1097/SLA.0000000000004644
83. Eltzschig HK, Bratton DL, Colgan SP. Targeting hypoxia signalling for the treatment of ischaemic and inflammatory diseases. *Nat Rev Drug Discov*. 2014;13:852-869.
84. Haase VH, Chertow GM, Block GA, et al. Effects of vadadustat on hemoglobin concentrations in patients receiving hemodialysis previously treated with erythropoiesis-stimulating agents. *Nephrol Dial Transplant*. 2019;34:90-99.
85. Chen N, Hao C, Liu BC, et al. Roxadustat Treatment For Anemia In Patients Undergoing Long-Term Dialysis. *N Engl J Med*. 2019;381:1011-1022.

SUPPORTING INFORMATION

Additional Supporting Information may be found online in the Supporting Information section.

How to cite this article: Vohwinkel CU, Coit EJ, Burns N, et al. Targeting alveolar-specific succinate dehydrogenase A attenuates pulmonary inflammation during acute lung injury. *The FASEB Journal*. 2021;35:e21468. https://doi.org/10.1096/fj.202002778R